Flutter of a Multicomponent Beam in a Supersonic Flow

Marco Amato*
University of Bologna, 40136 Bologna, Italy
Isaac Elishakoff†
Florida Atlantic University, Boca Raton, Florida 33431-0991
and
J. N. Reddy‡
Texas A&M University, College Station, Texas 77843-3127

https://doi.org/10.2514/1.J060631

This study is devoted to the investigation of flutter of beams with highly contrasting materials. Two versions of the Galerkin method are applied: original version and modified version. It is shown that the modified Galerkin method tends to the exact solution for the inhomogeneous case in contrast with the original implementation, which does not. Secondly, modified and original Galerkin methods tend to the same solution in the homogeneous case. As far as the flutter is concerned, the modified Galerkin method tends to the finite element solution for the inhomogeneous case in contrast with the original implementation, which does not. Both original and modified Galerkin methods in the inhomogeneous case require many more terms (namely, 300) than the modified Galerkin method in the homogeneous case, where 10 terms sufficient.

Downloaded by UNIVERSITA DI TRENTO on July 20, 2021 | http://arc.aiaa.org | DOI: 10.2514/1.J060631

Nomenclature

A_i	=	area of cross section i, m^2
$c_{\bowtie}$	=	velocity of sound in undisturbed gas, m/s
E_i	=	elastic modulus of material i, Pa
H	=	potential of the conservative forces, J
I_i	=	moment of inertia of cross section i, m^4
L	=	total length of the beam, m
L_i	=	length of span i, m
$p_{\bowtie}$	=	pressure in the undisturbed gas, Pa
T	=	kinetic energy of the system, J
t	=	time, s
U	=	velocity of sound in undisturbed gas, m/s
W_{nc}	=	virtual work of nonconservative forces, J
x	=	axial coordinate of the problem, m
κ	=	polytropy index
Π	=	potential total energy, J
ρ_i	=	mass density of material i, kg/m^2
Φ	=	elastic deformation energy, J
Ω	=	complex flexional frequency of beam vibration, rad/s

I. Introduction

THE flutter of elastic bodies has been a subject of several books. These are the books by Bisplinghoff et al. [1], Fung [2], Bolotin [3], Försching [4], Dowell [5], Librescu [6], Starossek [7], Hodges and Pierce [8], Wright and Cooper [9], Algazin and Kijko [10], and Bhat [11], and an all-time classic book by Dowell [12], the fifth edition of which appeared in 2015. The review articles by Dowell [13], Novichkov [14], Friedmann [15], Livne [16], Pettit [17], Dowell [18], and Beran et al. [19] ought to be mentioned. The present paper is devoted to study the flutter of beams made of materials with highly contrasting properties that appear in numerous applications in modern engineering, including in particular sandwich structures as photovoltaic panels [20] and laminated glass [21], energy harvesting devices [22], smart periodic structures [23], and acoustic metamaterial components [24]. Mechanics of such structures was studied in several recent papers. Specifically, Kaplunov et al. [25] and Kudaibergenov et al. [26] investigated vibrations of the two- and multicomponent strings.

In such circumstances, it is important to have knowledge of the lowest natural frequency of the structure, in order to avoid resonance. This topic was addressed in detail in recent studies conducted by Kaplunov et al. [27] and Şahin et al. [28]. Previous works that resonate with highly contrasting material structures were associated with the presence of the defect and attendant localization, as was done by Li et al. [29], Xie and Elishakoff [30], Zingales and Elishakoff [31], and Elishakoff et al. [32]. The definitive studies by Dugundji et al. [33], Fung [34], Kaza and Kielb [35], Parks [36], Dugundji [37], Gwin and Taylor [38], Pidaparti and Yang [39], and Zhang et al. [40] ought to be mentioned. Dowell and Bendiksen [41] summarized panel flutter's status by the year 2010. Combinations of turbulence and vibrations in supersonic flow were studied by Elishakoff and Kromatoff [42], Elishakoff [43], and Hashimoto et al. [44].

This paper deals with multicomponent beams; closest in spirit to this type of structures are two-, three-, and multispan beams. Free vibrations of two-span and three-span beams were studied by Veletsos and Newmark [45], Makhortykh [46], and Gorman [47]. Flutter of two-span beams was investigated by Makhortykh [48,49], whereas multispan beams were studied by Rodden [50], Dowell [51,52], and Song et al. [53].

This study is dealing with the flutter of multicomponent beams. We use two different versions of the Galerkin method: the original version and the modified one. Usually, the literature uses the original approach. Here we show that the interface between two materials ought to be written via generalized functions, namely, Heaviside function, Dirac's delta function, and doublet function. We illustrate that the use of the conventional, original version does not converge with finite element method (FEM) results for the flutter velocity. We show that one should use the modified version of the Galerkin method for flutter problems.

II. Governing Differential Equation of Flutter of a Multicomponent Beam

We are interested to solve the problem shown in Fig. 1: a multicomponent beam composed of three different elements.

Received 11 February 2021; revision received 31 March 2021; accepted for publication 7 April 2021; published online 19 July 2021. Copyright © 2021 by the American Institute of Aeronautics and Astronautics, Inc. All rights reserved. All requests for copying and permission to reprint should be submitted to CCC at www.copyright.com; employ the eISSN 1533-385X to initiate your request. See also AIAA Rights and Permissions www.aiaa.org/randp.

*M.Sc. Eng., Department of Civil, Chemical, Environmental, and Materials Engineering, Viale del Risorgimento 2; marco.amato@studio.unibo.it.

†Distinguished Research Professor, Department of Ocean and Mechanical Engineering; elishako@fau.edu.

‡O'Donnell Foundation Chair IV Professor, Regents Professor, and University Distinguished Professor; J. Mike Walker '66 Department of Mechanical Engineering; jnreddy@tamu.edu.

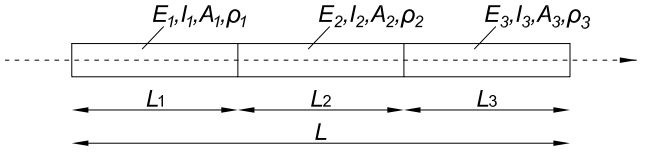

Fig. 1 A multicomponent beam of length L.

In Fig. 1, E_1, E_2, and E_3 denote the elastic modulus of the related element; I_1, I_2, and I_3 denote the associated moments of inertia of the cross section; A_1, A_2, and A_3 denote the cross-sectional areas of the span; ρ_1, ρ_2, and ρ_3 denote the mass density of the span material; and L_1, L_2, and L_3 denote the lengths of the relevant portion.

In our case, we deal with a multicomponent beam. In that way the cross section remains the same and the result is that $I_1 = I_2 = I_3$ and $A_1 = A_2 = A_3$.

The governing differential equation for the flutter problem reads as follows:

$$\frac{\partial^2}{\partial x^2}\left(E(x)I(x)\frac{\partial^2 w}{\partial x^2}\right) + \rho(x)A(x)\frac{\partial^2 w}{\partial t^2} + q(x,t) = 0 \tag{1}$$

where $q(x, t)$ represent the load from piston theory of a gas flow.

The piston theory load is analyzed in the following formula proposed by Bolotin [3]:

$$q(x,t) = Pb = \frac{\kappa p_{\triangleright\!\triangleleft} b}{c_{\triangleright\!\triangleleft}}\left(\frac{\partial w}{\partial t} + U\frac{\partial w}{\partial x}\right) \tag{2}$$

where κ is the polytropy index of the gas, $p_{\triangleright\!\triangleleft}$ is the pressure (in the undisturbed gas), $c_{\triangleright\!\triangleleft}$ is the velocity of sound in the undisturbed gas, and U is the velocity of gas flow.

$$\frac{\partial^2}{\partial x^2}\left(E(x)I(x)\frac{\partial^2 w}{\partial x^2}\right) + \rho(x)A(x)\frac{\partial^2 w}{\partial t^2} + \frac{\kappa p_{\triangleright\!\triangleleft} b}{c_{\triangleright\!\triangleleft}}\left(\frac{\partial w}{\partial t} + U\frac{\partial w}{\partial x}\right) = 0 \tag{3}$$

or

$$\frac{\partial^2}{\partial x^2}\left(E(x)I(x)\frac{\partial^2 w}{\partial x^2}\right) + \rho(x)A(x)\frac{\partial^2 w}{\partial t^2} + \frac{\kappa p_{\triangleright\!\triangleleft} b}{c_{\triangleright\!\triangleleft}}\frac{\partial w}{\partial t} + \frac{\kappa p_{\triangleright\!\triangleleft} bU}{c_{\triangleright\!\triangleleft}}\frac{\partial w}{\partial x} = 0 \tag{4}$$

For each step,

$$E_i I_i \frac{\partial^4 w}{\partial x^4} + \rho_i A_i \frac{\partial^2 w}{\partial t^2} + \frac{\kappa p_{\triangleright\!\triangleleft} b}{c_{\triangleright\!\triangleleft}}\frac{\partial w}{\partial t} + \frac{\kappa p_{\triangleright\!\triangleleft} bU}{c_{\triangleright\!\triangleleft}}\frac{\partial w}{\partial x} = 0 \tag{5}$$

III. Exact Solution

Thinking $w(x, t)$ as

$$w(x,t) = e^{rx}e^{\Omega t} \tag{6}$$

where r is a characteristic exponent and Ω is a complex eigenfrequency, we obtain

$$E_i I_i r^4 + \rho_i A_i \Omega^2 + \frac{\kappa p_{\triangleright\!\triangleleft} b}{c_{\triangleright\!\triangleleft}}\Omega + \frac{\kappa p_{\triangleright\!\triangleleft} bU}{c_{\triangleright\!\triangleleft}} r = 0 \tag{7}$$

or

$$E_i I_i r^4 + \frac{\kappa p_{\triangleright\!\triangleleft} bU}{c_{\triangleright\!\triangleleft}} r - \lambda_i = 0 \tag{8}$$

where λ_i is defined as follows:

$$\lambda_i = -\left(\rho_i A_i \Omega^2 + \frac{\kappa p_{\triangleright\!\triangleleft} b}{c_{\triangleright\!\triangleleft}}\Omega\right) \tag{9}$$

Thinking the first two roots of Eq. (8) as

$$r_{1,2} = \mu \pm i\beta \tag{10}$$

we can divide Eq. (8) by

$$(r - r_1)(r - r_2) \tag{11}$$

or, substituting the meaning of Eq. (10),

$$r^2 - 2\mu r + \mu^2 + \beta^2 \tag{12}$$

to define the last two roots.

The ratio of Eq. (8) by Eq. (12) leads us to the quotient $E_i I_i r^2 + 2E_i I_i \mu r + E_i I_i(3\mu^2 - \beta^2)$, with as a reminder $((\kappa p_{\triangleright\!\triangleleft} bU/c_{\triangleright\!\triangleleft}) + 4E_i I_i \mu^3 - 4E_i I_i \mu\beta^2)r - \lambda_i - E_i I_i(\mu^2 + \beta^2)(3\mu^2 - \beta^2)$. To be a divisor, the reminder must vanish, which leads us to the following system:

$$\begin{cases} \frac{\kappa p_{\triangleright\!\triangleleft} bU}{c_{\triangleright\!\triangleleft}} + 4E_i I_i \mu^3 - 4E_i I_i \mu\beta^2 = 0 \\ -\lambda_i - E_i I_i(\mu^2 + \beta^2)(3\mu^2 - \beta^2) = 0 \end{cases} \tag{13}$$

From this system we can define $(\kappa p_{\triangleright\!\triangleleft} bU/c_{\triangleright\!\triangleleft})$ and λ_i:

$$\begin{cases} \frac{\kappa p_{\triangleright\!\triangleleft} bU}{c_{\triangleright\!\triangleleft}} = 4E_i I_i \mu(\beta^2 - \mu^2) \\ \lambda_i = E_i I_i(\mu^2 + \beta^2)(\beta^2 - 3\mu^2) \end{cases} \tag{14}$$

The last two roots of Eq. (8), namely, r_3 and r_4, are the roots of the ratio. We can obtain them as follows:

$$E_i I_i r^2 + 2E_i I_i \mu r + E_i I_i(3\mu^2 - \beta^2) = 0 \tag{15a}$$

$$r^2 + 2\mu r + 3\mu^2 - \beta^2 = 0 \tag{15b}$$

$$r_{3,4} = \frac{-2\mu \pm \sqrt{-8\mu^2 + 4\beta^2}}{2} \tag{15c}$$

$$r_{3,4} = -\mu \pm \sqrt{-2\mu^2 + \beta^2} \tag{15d}$$

We assumed that $w(x, t) = W(x)T(t)$, where the spatial part is e^{rx}. Moreover, we found out that we have four values for the characteristic exponent, as a conclusion:

$$W_i(x) = e^{r_{1,i}x} + e^{r_{2,i}x} + e^{r_{3,i}x} + e^{r_{4,i}x} \tag{16}$$

With the obtained roots we can define the system of equations that define the problem:

$$W_1(0) = 0 \tag{17a}$$

$$W_1''(0) = 0 \tag{17b}$$

$$W_1(x_1) = W_2(x_1) \tag{17c}$$

$$W_1'(x_1) = W_2'(x_1) \tag{17d}$$

$$E_1 I_1 W_1''(x_1) = E_2 I_2 W_2''(x_1) \tag{17e}$$

$$E_1 I_1 W_1'''(x_1) = E_2 I_2 W_2'''(x_1) \tag{17f}$$

$$W_2(x_2) = W_3(x_2) \tag{17g}$$

$$W_2'(x_2) = W_3'(x_2) \tag{17h}$$

Downloaded by UNIVERSITA DI TRENTO on July 20, 2021 | http://arc.aiaa.org | DOI: 10.2514/1.J060631

$$E_2 I_2 W_2''(x_2) = E_3 I_3 W_3''(x_2) \tag{17i}$$

$$E_2 I_2 W_2'''(x_2) = E_3 I_3 W_3'''(x_2) \tag{17j}$$

$$W_3(L) = 0 \tag{17k}$$

$$W_3''(L) = 0 \tag{17l}$$

We can rewrite this system of equation in a matrix form (defined matrix $\boldsymbol{P}$), and after that we substitute the meaning of the four roots. This is a homogeneous system and it has nontrivial solution only when the determinant of $\boldsymbol{P}$ is equal to zero. This determinant depends on the parameters μ_i, β_i for each portion of the beam. As a result, the final system that allows us to solve the flutter problem reads

$$\det(\boldsymbol{P}(\mu_1, \beta_1, \mu_2, \beta_2, \mu_3, \beta_3)) = 0 \tag{18a}$$

$$\frac{\kappa p_{\triangleright\!\triangleleft} b_1 U}{c_{\triangleright\!\triangleleft}} = 4E_1 I_1 \mu_1 (\beta_1^2 - \mu_1^2) \tag{18b}$$

$$\frac{\kappa p_{\triangleright\!\triangleleft} b_2 U}{c_{\triangleright\!\triangleleft}} = 4E_2 I_2 \mu_2 (\beta_2^2 - \mu_2^2) \tag{18c}$$

$$\frac{\kappa p_{\triangleright\!\triangleleft} b_3 U}{c_{\triangleright\!\triangleleft}} = 4E_3 I_3 \mu_3 (\beta_3^2 - \mu_3^2) \tag{18d}$$

$$\lambda_1 = E_1 I_1 (\mu_1^2 + \beta_1^2)(\beta_1^2 - 3\mu_1^2) \tag{18e}$$

$$\lambda_2 = E_2 I_2 (\mu_2^2 + \beta_2^2)(\beta_2^2 - 3\mu_2^2) \tag{18f}$$

$$\lambda_3 = E_3 I_3 (\mu_3^2 + \beta_3^2)(\beta_3^2 - 3\mu_3^2) \tag{18g}$$

We are supposed to know all the parameters related to the beam and to the gas flow. With this assumption we obtain seven unknowns for seven equations: the nonlinear system is solvable. The unknowns are the six parameters related to the three characteristic exponents $\mu_1, \beta_1, \mu_2, \beta_2, \mu_3, \beta_3$ and the eigenfrequency Ω, which are inside λ_i.

The nonlinear system composed of Eqs. (18a–18g) is too big to be solved analytically, so we need a different solution for the stepped beam. On the other hand, if our beam is homogeneous and uniform a solution can be obtained because we do not need compatibility conditions and the system is in the following simpler form:

$$\det(\boldsymbol{P}(\mu_1, \beta_1)) = 0 \tag{19a}$$

$$\frac{\kappa p_{\triangleright\!\triangleleft} b_1 U}{c_{\triangleright\!\triangleleft}} = 4E_1 I_1 \mu_1 (\beta_1^2 - \mu_1^2) \tag{19b}$$

$$\lambda_1 = E_1 I_1 (\mu_1^2 + \beta_1^2)(\beta_1^2 - 3\mu_1^2) \tag{19c}$$

IV. Application of the Finite Element Method

To obtain a reference solution for the two different implementations of the Galerkin method, we implement our finite element method code. The finite element method applied on structures subject to gas flow is not a new method. In fact, it was already used, for example, by Marzani et al. [54], Olson [55], Olson and Jamison [56], Kock and Olson [57], Pramila et al. [58], and Ryu et al. [59]. We use the variational approach starting on Hamilton's principle, which reads

$$\int_{t_1}^{t_2} \delta(T - \Pi)\, \mathrm{d}t + \int_{t_1}^{t_2} \delta W_{\mathrm{nc}}\, \mathrm{d}t = 0 \tag{20}$$

denoting Π, the potential total energy of the system as

$$\Pi = \Phi + H \tag{21}$$

where Φ is the elastic deformation energy of the system, H is the potential of the conservative forces, T is the kinetic energy of the system, and W_{nc} is the virtual work of nonconservative forces.

According to Hamilton's principle, and for the one-dimensional system under study, we can say that the difference between the variations of kinetic energy T and potential energy Π added to the variation of virtual work of nonconservative forces into any time interval $[t_1 - t_2]$ must be equal to zero.

Because of a configuration change, the energetical terms and the work terms take the following form:

Elastic potential energy of the beam:

$$\Phi = \frac{1}{2}\int_0^L EI\left(\frac{\partial^2 w}{\partial x^2}\right)^2 \mathrm{d}x \tag{22}$$

Kinetic energy:

$$T = \frac{1}{2}\int_0^L \rho A\left(\frac{\partial w}{\partial t}\right)^2 \mathrm{d}x \tag{23}$$

Virtual work of nonconservative forces:

$$\delta W_{\mathrm{nc}} = -\int_0^L q(x,t)\delta w\, \mathrm{d}x \tag{24}$$

Substituting in Eq. (24) the meaning of piston theory nonconservative forces (2), we obtain

$$\delta W_{\mathrm{nc}} = -\int_0^L \frac{\kappa p_{\triangleright\!\triangleleft} b}{c_{\triangleright\!\triangleleft}}\left(\frac{\partial w}{\partial t} + U\frac{\partial w}{\partial x}\right)\delta w\, \mathrm{d}x \tag{25}$$

or

$$\delta W_{\mathrm{nc}} = -\int_0^L \frac{\kappa p_{\triangleright\!\triangleleft} b}{c_{\triangleright\!\triangleleft}}\frac{\partial w}{\partial t}\delta w\, \mathrm{d}x - \int_0^L \frac{\kappa p_{\triangleright\!\triangleleft} b}{c_{\triangleright\!\triangleleft}} U\frac{\partial w}{\partial x}\delta w\, \mathrm{d}x \tag{26}$$

Now we evaluate the variations of quantities (22) and (23):

$$\delta\Phi = \int_0^L EI\frac{\partial^2 w}{\partial x^2}\delta\left(\frac{\partial^2 w}{\partial x^2}\right)\mathrm{d}x \tag{27}$$

$$\delta T = \int_0^L \rho A\frac{\partial w}{\partial t}\delta\left(\frac{\partial w}{\partial t}\right)\mathrm{d}x \tag{28}$$

Substituting Eqs. (27), (28), and (26) into Eq. (21) and, in conclusion, into Eq. (20), we obtain

$$\int_{t_1}^{t_2}\left[\int_0^L \rho A\frac{\partial w}{\partial t}\delta\left(\frac{\partial w}{\partial t}\right)x\right]\mathrm{d}t - \int_{t_1}^{t_2}\left[\int_0^L EI\frac{\partial^2 w}{\partial x^2}\delta\left(\frac{\partial^2 w}{\partial x^2}\right)\mathrm{d}x\right]\mathrm{d}t - \int_{t_1}^{t_2}\left[\int_0^L \frac{\kappa p_{\triangleright\!\triangleleft} b}{c_{\triangleright\!\triangleleft}}\frac{\partial w}{\partial t}\delta w\, \mathrm{d}x + \int_0^L \frac{\kappa p_{\triangleright\!\triangleleft} b}{c_{\triangleright\!\triangleleft}} U\frac{\partial w}{\partial x}\delta w\, \mathrm{d}x\right]\mathrm{d}t = 0 \tag{29}$$

Integration by part of first term leads us to

$$\int_0^L\left[\int_{t_1}^{t_2} \rho A\frac{\partial w}{\partial t}\delta\left(\frac{\partial w}{\partial t}\right)\mathrm{d}t\right]\mathrm{d}x = \int_0^L\left[\rho A\frac{\partial w}{\partial t}\delta w\right]_{t_1}^{t_2}\mathrm{d}x - \int_0^L\left\{\int_{t_1}^{t_2}\left[\rho A\frac{\partial^2 w}{\partial t^2}\delta w\right]\mathrm{d}t\right\}\mathrm{d}x \tag{30}$$

We can switch the integration order because the length of the system does not change in time.

Because we use the assumption of *synchronous varied motions*, we have $\delta w(x, t_1) = \delta w(x, t_2) = 0$. As a conclusion, Eq. (30) becomes

Downloaded by UNIVERSITA DI TRENTO on July 20, 2021 | http://arc.aiaa.org | DOI: 10.2514/1.J060631

$$\int_0^L \left[\int_{t_1}^{t_2} \rho A \frac{\partial w}{\partial t} \delta\left(\frac{\partial w}{\partial t}\right) \mathrm{d}t \right] \mathrm{d}x = -\int_0^L \left\{ \int_{t_1}^{t_2} \left[\rho A \frac{\partial^2 w}{\partial t^2} \delta w \right] \mathrm{d}t \right\} \mathrm{d}x \tag{31}$$

The request of a variational formulation valid for each time interval $[t_1 - t_2]$ demands that the integrand of Eq. (29) vanishes. In addition, using Eq. (31), Hamilton's principle can be rewritten as

$$\int_0^L \rho A \frac{\partial^2 w}{\partial t^2} \delta w \, \mathrm{d}x + \int_0^L EI \frac{\partial^2 w}{\partial x^2} \delta\left(\frac{\partial^2 w}{\partial x^2}\right) \mathrm{d}x + \int_0^L \frac{\kappa p_{\triangleright\!\triangleleft} b}{c_{\triangleright\!\triangleleft}} \frac{\partial w}{\partial t} \delta w \, \mathrm{d}x + \int_0^L \frac{\kappa p_{\triangleright\!\triangleleft} b}{c_{\triangleright\!\triangleleft}} U \frac{\partial w}{\partial x} \delta w \, \mathrm{d}x = 0 \tag{32}$$

Now, subdividing the whole domain in n elements, the length of each element becomes

$$L_e = \frac{L}{n} \tag{33}$$

The local coordinate $\overline{x}$ of each element, in particular for the ith element reads as follows:

$$\overline{x} = x - (i-1)L_e \tag{34}$$

With considerations (34) and (33), we can rewrite Eq. (32) as follows:

$$\sum_{i=1}^{n} \left[\int_0^{L_e} \rho A \frac{\partial^2 w}{\partial t^2} \delta w \, \mathrm{d}\overline{x} + \int_0^{L_e} EI \frac{\partial^2 w}{\partial \overline{x}^2} \delta\left(\frac{\partial^2 w}{\partial \overline{x}^2}\right) \mathrm{d}\overline{x} + \int_0^{L_e} \frac{\kappa p_{\triangleright\!\triangleleft} b}{c_{\triangleright\!\triangleleft}} \frac{\partial w}{\partial t} \delta w \, \mathrm{d}\overline{x} + \int_0^{L_e} \frac{\kappa p_{\triangleright\!\triangleleft} b}{c_{\triangleright\!\triangleleft}} U \frac{\partial w}{\partial \overline{x}} \delta w \, \mathrm{d}\overline{x} \right] = 0 \tag{35}$$

We can also introduce the following dimensionless coordinate in order to reduce the analytical complexity:

$$v = \frac{w}{L_e} \rightarrow w = vL_e \tag{36a}$$

$$\xi = \frac{\overline{x}}{L_e} \rightarrow \overline{x} = \xi L_e \tag{36b}$$

Equation (35) with considerations (36a) and (36b) becomes

$$\sum_{i=1}^{n} \left[\int_0^1 \rho A L_e^3 \frac{\partial^2 v}{\partial t^2} \delta v \, \mathrm{d}\xi + \int_0^1 \frac{EI}{L_e} \frac{\partial^2 v}{\partial \xi^2} \delta\left(\frac{\partial^2 v}{\partial \xi^2}\right) \mathrm{d}\xi + \int_0^1 \frac{\kappa p_{\triangleright\!\triangleleft} b}{c_{\triangleright\!\triangleleft}} L_e^3 \frac{\partial v}{\partial t} \delta v \, \mathrm{d}\xi + \int_0^1 \frac{\kappa p_{\triangleright\!\triangleleft} b}{c_{\triangleright\!\triangleleft}} U L_e^2 \frac{\partial v}{\partial \xi} \delta v \, \mathrm{d}\xi \right] = 0 \tag{37}$$

The displacement field of a Bernoulli–Euler finite element is described in four components, two for each end: two translations $w_1 = w_1(t)$ and $w_2 = w_2(t)$ and two rotations $\varphi_1 = \varphi_1(t)$ and $\varphi_2 = \varphi_2(t)$.

With those assumptions the displacement field is defined as follows:

$$w(\overline{x}, t) = N_1(\overline{x}) w_1(t) + N_2(\overline{x}) \varphi_1(t) + N_3(\overline{x}) w_2(t) + N_4(\overline{x}) \varphi_2(t) \tag{38}$$

Equation (38) is the linear combination of shape functions $N_i(\overline{x})(i = 1, 2, 3, 4)$ with the displacement fields $w_1(t)$, $\varphi_1(t)$, $w_2(t)$, and $\varphi_2(t)$.

Differential equation (5) shows that the function $w(\overline{x}, t)$ must be differentiable until four times, which requires polynomial shape functions of third order as follows:

$$N_1 = N_1(\overline{x}) = 1 - 3\frac{\overline{x}^2}{L_e^2} + 2\frac{\overline{x}^3}{L_e^3} \tag{39a}$$

$$N_2 = N_2(\overline{x}) = -\overline{x} + 2\frac{\overline{x}^2}{L_e} - \frac{\overline{x}^3}{L_e^2} \tag{39b}$$

$$N_3 = N_3(\overline{x}) = 3\frac{\overline{x}^2}{L_e^2} - 2\frac{\overline{x}^3}{L_e^3} \tag{39c}$$

$$N_4 = N_4(\overline{x}) = \frac{\overline{x}^2}{L_e} - \frac{\overline{x}^3}{L_e^2} \tag{39d}$$

Equations (39a–39d) with consideration (36b) take the following form:

$$N_1 = N_1(\xi) = 1 - 3\xi^2 + 2\xi^3 \tag{40a}$$

$$N_2 = N_2(\xi) = L_e(-\xi + 2\xi^2 - \xi^3) \tag{40b}$$

$$N_3 = N_3(\xi) = 3\xi^2 - 2\xi^3 \tag{40c}$$

$$N_4 = N_4(\xi) = L_e(\xi^2 - \xi^3) \tag{40d}$$

Thanks to Eqs. (40a–40d) the variable $w(\xi, t)$ takes the followings form:

$$w(\xi, t) = N_1(\xi) w_1(t) + N_2(\xi) \varphi_1(t) + N_3(\xi) w_2(t) + N_4(\xi) \varphi_2(t) \tag{41}$$

The dimensionless variable $v = v(\xi, t)$, with considerations (36a) and (41), can be expressed in the following form:

$$v(\xi, t) = \frac{w(\xi, t)}{L_e} = \frac{1}{L_e} N_1(\xi) w_1(t) + \frac{1}{L_e} N_2(\xi) \varphi_1(t) + \frac{1}{L_e} N_3(\xi) w_2(t) + \frac{1}{L_e} N_4(\xi) \varphi_2(t) \tag{42}$$

Introducing the following notations:

$$\overline{N}_1 = \frac{1}{L_e} N_1(\xi) = \frac{1}{L_e}(1 - 3\xi^2 + 2\xi^3) \tag{43a}$$

$$\overline{N}_2 = \frac{1}{L_e} N_2(\xi) = -\xi + 2\xi^2 - \xi^3 \tag{43b}$$

$$\overline{N}_3 = \frac{1}{L_e} N_3(\xi) = \frac{1}{L_e}(3\xi^2 - 2\xi^3) \tag{43c}$$

$$\overline{N}_4 = \frac{1}{L_e} N_4(\xi) = \xi^2 - \xi^3 \tag{43d}$$

and defining with $\boldsymbol{N}$ the shape functions vector and with $\boldsymbol{u}$ the nodal displacements vector as follows:

$$\boldsymbol{N} = \boldsymbol{N}(\xi) = [\overline{N}_1(\xi) \overline{N}_2(\xi) \overline{N}_3(\xi) \overline{N}_4(\xi)]^T \tag{44}$$

$$\boldsymbol{u} = \boldsymbol{u}(t) = [w_1(t) \varphi_1(t) w_2(t) \varphi_2(t)]^T \tag{45}$$

by considering (44) and (45), Eq. (42) takes the following form:

$$v(\xi, t) = \boldsymbol{N}^T(\xi) \boldsymbol{u}(t) = \boldsymbol{u}^T(t) \boldsymbol{N}(\xi) \tag{46}$$

In Eq. (37) we have the first and second derivatives of variable $v(\xi, t)$ with respect to dimensionless coordinate ξ.

Downloaded by UNIVERSITA DI TRENTO on July 20, 2021 | http://arc.aiaa.org | DOI: 10.2514/1.J060631

Downloaded by UNIVERSITA DI TRENTO on July 20, 2021 | http://arc.aiaa.org | DOI: 10.2514/1.J060631

The first derivative can be written as follows:

$$v'(\xi,t)=\frac{\partial v(\xi,t)}{\partial\xi}=\overline{N}_1'(\xi)w_1(t)+\overline{N}_2'(\xi)\varphi_1(t)+\overline{N}_3'(\xi)w_2(t)+\overline{N}_4'(\xi)\varphi_2(t) \tag{47}$$

with

$$\overline{N}_1'(\xi)=\frac{d\overline{N}_1(\xi)}{d\xi}=\frac{1}{L_e}(-6\xi+6\xi^2) \tag{48a}$$

$$\overline{N}_2'(\xi)=\frac{d\overline{N}_2(\xi)}{d\xi}=-1+4\xi-3\xi^2 \tag{48b}$$

$$\overline{N}_3'(\xi)=\frac{d\overline{N}_3(\xi)}{d\xi}=\frac{1}{L_e}(6\xi-6\xi^2) \tag{48c}$$

$$\overline{N}_4'(\xi)=\frac{d\overline{N}_4(\xi)}{d\xi}=2\xi-3\xi^2 \tag{48d}$$

Denoting with $\boldsymbol{D}$ the vector of the first derivative of shape functions, we have

$$\boldsymbol{D}=\frac{d}{d\xi}[\overline{N}_1(\xi)\overline{N}_2(\xi)\overline{N}_3(\xi)\overline{N}_4(\xi)]^T=[\overline{N}_1'(\xi)\overline{N}_2'(\xi)\overline{N}_3'(\xi)\overline{N}_4'(\xi)]^T=\frac{d}{d\xi}\boldsymbol{N}(\xi) \tag{49}$$

Equation (47) becomes

$$v'(\xi,t)=\boldsymbol{D}^T(\xi)\boldsymbol{u}(t)=\boldsymbol{u}^T(t)\boldsymbol{D}(\xi) \tag{50}$$

Analogously, we can define the second derivative:

$$v''(\xi,t)=\frac{\partial^2 v(\xi,t)}{\partial\xi^2}=\overline{N}_1''(\xi)w_1(t)+\overline{N}_2''(\xi)\varphi_1(t)+\overline{N}_3''(\xi)w_2(t)+\overline{N}_4''(\xi)\varphi_2(t) \tag{51}$$

with

$$\overline{N}_1''(\xi)=\frac{d^2\overline{N}_1(\xi)}{d\xi^2}=\frac{1}{L_e}(-6+12\xi) \tag{52a}$$

$$\overline{N}_2''(\xi)=\frac{d^2\overline{N}_2(\xi)}{d\xi^2}=4\xi-6\xi \tag{52b}$$

$$\overline{N}_3''(\xi)=\frac{d^2\overline{N}_3(\xi)}{d\xi^2}=\frac{1}{L_e}(6-12\xi) \tag{52c}$$

$$\overline{N}_4''(\xi)=\frac{d^2\overline{N}_4(\xi)}{d\xi^2}=2-6\xi \tag{52d}$$

Denoting with $\boldsymbol{B}$ the vector of the second derivative of shape functions, we have

$$\boldsymbol{B}=\frac{d^2}{d\xi^2}[\overline{N}_1(\xi)\overline{N}_2(\xi)\overline{N}_3(\xi)\overline{N}_4(\xi)]^T=[\overline{N}_1''(\xi)\overline{N}_2''(\xi)\overline{N}_3''(\xi)\overline{N}_4''(\xi)]^T=\frac{d^2}{d\xi^2}\boldsymbol{N}(\xi) \tag{53}$$

Equation (51) becomes

$$v''(\xi,t)=\boldsymbol{B}^T(\xi)\boldsymbol{u}(t)=\boldsymbol{u}^T(t)\boldsymbol{B}(\xi) \tag{54}$$

We also have, in Eq. (37), the second derivative with respect to time of variable $v(\xi,t)$. That derivative can be written as follows:

$$\ddot{v}(\xi,t)=\frac{\partial^2 v(\xi,t)}{\partial t^2}=\overline{N}_1(\xi)\ddot{w}_1(t)+\overline{N}_2(\xi)\ddot{\varphi}_1(t)+\overline{N}_3(\xi)\ddot{w}_2(t)+\overline{N}_4(\xi)\ddot{\varphi}_2(t) \tag{55}$$

or

$$\ddot{v}(\xi,t)=\boldsymbol{N}^T(\xi)\ddot{\boldsymbol{u}}(t)=\ddot{\boldsymbol{u}}^T(t)\boldsymbol{N}(\xi) \tag{56}$$

Introducing Eqs. (46), (50), (54), and (56) into Eq. (37), we obtain

$$\sum_{i=1}^{n}\left[\int_0^1\delta(\boldsymbol{u}^T\boldsymbol{N})\rho AL_e^3\boldsymbol{N}^T\ddot{\boldsymbol{u}}\,\mathrm{d}\xi+\int_0^1\delta(\boldsymbol{u}^T\boldsymbol{B})\frac{EI}{L_e}\boldsymbol{B}^T\boldsymbol{u}\,\mathrm{d}\xi+\int_0^1\delta(\boldsymbol{u}^T\boldsymbol{N})\frac{\kappa p_{\triangleright\!\triangleleft}b}{c_{\triangleright\!\triangleleft}}L_e^3\boldsymbol{N}^T\dot{\boldsymbol{u}}\,\mathrm{d}\xi+\int_0^1\delta(\boldsymbol{u}^T\boldsymbol{N})\frac{\kappa p_{\triangleright\!\triangleleft}b}{c_{\triangleright\!\triangleleft}}UL_e^2\boldsymbol{D}^T\boldsymbol{u}\,\mathrm{d}\xi\right]=\boldsymbol{0} \tag{57}$$

Because the vector $\boldsymbol{u}$ is a function only of time, we can take it out of the integral sign:

$$\sum_{i=1}^{n}\delta(\boldsymbol{u}^T)\left[\int_0^1\boldsymbol{N}\rho AL_e^3\boldsymbol{N}^T\,\mathrm{d}\xi\ddot{\boldsymbol{u}}+\int_0^1\boldsymbol{B}\frac{EI}{L_e}\boldsymbol{B}^T\,\mathrm{d}\xi\boldsymbol{u}+\int_0^1\boldsymbol{N}\frac{\kappa p_{\triangleright\!\triangleleft}b}{c_{\triangleright\!\triangleleft}}L_e^3\boldsymbol{N}^T\,\mathrm{d}\xi\dot{\boldsymbol{u}}+\int_0^1\boldsymbol{N}\frac{\kappa p_{\triangleright\!\triangleleft}b}{c_{\triangleright\!\triangleleft}}UL_e^2\boldsymbol{D}^T\,\mathrm{d}\xi\boldsymbol{u}\right]=\boldsymbol{0} \tag{58}$$

Denoting a) element mass matrix $\boldsymbol{m}=m_{ij}$ as follows:

$$\boldsymbol{m}=\int_0^1\boldsymbol{N}\rho AL_e^3\boldsymbol{N}^T\,\mathrm{d}\xi \tag{59}$$

or

$$m_{ij}=\int_0^1 N_i\rho AL_e^3N_j\,\mathrm{d}\xi \tag{60}$$

b) element stiffness matrix $\boldsymbol{k}=k_{ij}$ as follows:

$$\boldsymbol{k}=\int_0^1\boldsymbol{B}\frac{EI}{L_e}\boldsymbol{B}^T\,\mathrm{d}\xi \tag{61}$$

or

$$k_{ij}=\int_0^1 B_i\frac{EI}{L_e}B_j\,\mathrm{d}\xi \tag{62}$$

c) aerodynamic damping matrix $\boldsymbol{q}_1=q_{1ij}$ as follows:

$$\boldsymbol{q}_1=\int_0^1\boldsymbol{N}\frac{\kappa p_{\triangleright\!\triangleleft}b}{c_{\triangleright\!\triangleleft}}L_e^3\boldsymbol{N}^T\,\mathrm{d}\xi \tag{63}$$

or

$$q_{1ij}=\int_0^1 N_i\frac{\kappa p_{\triangleright\!\triangleleft}b}{c_{\triangleright\!\triangleleft}}L_e^3N_j\,\mathrm{d}\xi \tag{64}$$

and d) velocity load matrix $\boldsymbol{q}_2=q_{2ij}$ as follows:

$$\boldsymbol{q}_2=\int_0^1\boldsymbol{N}\frac{\kappa p_{\triangleright\!\triangleleft}b}{c_{\triangleright\!\triangleleft}}UL_e^2\boldsymbol{D}^T\,\mathrm{d}\xi \tag{65}$$

or

$$q_{2ij} = \int_0^1 N_i \frac{\kappa p_{\triangleright\triangleleft} b}{c_{\triangleright\triangleleft}} U L_e^2 D_j \, \mathrm{d}\xi \tag{66}$$

Equation (58) becomes

$$\sum_{i=1}^{n} \delta(\boldsymbol{u}^T)[\boldsymbol{m}\ddot{\boldsymbol{u}} + \boldsymbol{k}\boldsymbol{u} + \boldsymbol{q}_1\dot{\boldsymbol{u}} + \boldsymbol{q}_2\boldsymbol{u}] = \boldsymbol{0} \tag{67}$$

After a standard assembly procedure, we obtain

$$\delta\boldsymbol{v}^T(\boldsymbol{M}\ddot{\boldsymbol{v}} + \boldsymbol{K}\boldsymbol{v} + \boldsymbol{Q}_1\dot{\boldsymbol{v}} + \boldsymbol{Q}_2\boldsymbol{v}) = \boldsymbol{0} \tag{68}$$

where $\boldsymbol{M}$ is the global mass matrix of the system, $\boldsymbol{K}$ is the global stiffness matrix of the system, $\boldsymbol{Q}_1$ is the global aerodynamic damping matrix of the system, $\boldsymbol{Q}_2$ is the global velocity load matrix of the system, and $\boldsymbol{v}$ is the global nodal displacements vector of the system.

Adding the terms with each multiplied by $\boldsymbol{v}$, we obtain

$$\delta\boldsymbol{v}^T(\boldsymbol{M}\ddot{\boldsymbol{v}} + \boldsymbol{Q}_1\dot{\boldsymbol{v}} + \boldsymbol{Z}\boldsymbol{v}) = \boldsymbol{0} \tag{69}$$

where

$$\boldsymbol{Z} = \boldsymbol{K} + \boldsymbol{Q}_2 \tag{70}$$

To obtain a solution that is valid for each variation $\delta\boldsymbol{v}^T$, the terms within parentheses in Eq. (69) must vanish:

$$\boldsymbol{M}\ddot{\boldsymbol{v}} + \boldsymbol{Q}_1\dot{\boldsymbol{v}} + \boldsymbol{Z}\boldsymbol{v} = \boldsymbol{0} \tag{71}$$

Defining, now, $\boldsymbol{v}(t)$ as

$$\boldsymbol{v}(t) = \boldsymbol{V}e^{\Omega t} \tag{72}$$

we obtain

$$\Omega^2\boldsymbol{M}\boldsymbol{v} + \Omega\boldsymbol{Q}_1\boldsymbol{v} + \boldsymbol{Z}\boldsymbol{v} = \boldsymbol{0} \tag{73}$$

Collecting $\boldsymbol{v}(t)$, we get

$$(\Omega^2\boldsymbol{M} + \Omega\boldsymbol{Q}_1 + \boldsymbol{Z})\boldsymbol{v} = \boldsymbol{0} \tag{74}$$

Equation (74) is a homogeneous linear system in the parameter Ω. That system has nontrivial solution only when the determinant of the coefficient matrix (the terms inside parentheses) is equal to zero. Now the problem is to find the value of Ω that leads the determinant to zero:

$$\det(\Omega^2\boldsymbol{M} + \Omega\boldsymbol{Q}_1 + \boldsymbol{Z}) = 0 \tag{75}$$

V. Application of the Original Galerkin Method

Differential Eq. (5) can be solved with the well-known weighted residual method proposed by Galerkin in 1915. To apply the Galerkin procedure, we have, at first, to approximate the variable $w(x, t)$ by a series expansion, following Bolotin ([3], p. 248), Algazin and Kijko [10], and Dowell [12]:

$$w(x, t) = \sum_{k=1}^{n} Q_k \psi_k(x) f_k(t) \tag{76}$$

where $\psi_k(x)$ is a function of the nondimensional axial coordinate and $f_k(t)$ of nondimensional time t.

We consider the following variation of the function $f_k(t)$ in nondimensional time:

$$f_k(t) = e^{\Omega t} \tag{77}$$

We multiply the expression resulting from the substitution of Eq. (77) into Eq. (5) by $\psi_j(x)$ and integrate from zero to total length with respect of x:

$$\int_0^L \sum_{i=1}^{3}\left(\sum_{k=1}^{n} Q_k\left(E_i I_i \frac{d^4\psi_k(x)}{dx^4}\psi_j(x) + \frac{\kappa p_{\triangleright\triangleleft} bU}{c_{\triangleright\triangleleft}}\frac{d\psi_k(x)}{dx}\psi_j(x) + \Omega^2\rho_i A_i\psi_k(x)\psi_j(x) + \Omega\frac{\kappa p_{\triangleright\triangleleft} b}{c_{\triangleright\triangleleft}}\psi_k(x)\psi_j(x)\right)\right)\mathrm{d}x = 0 \tag{78}$$

After some algebra,

$$\sum_{k=1}^{n} Q_k\left(\sum_{i=1}^{3}\left[E_i I_i \int_{x_i}^{x_{i+1}} \frac{d^4\psi_k(x)}{dx^4}\psi_j(x)\,\mathrm{d}x\right] + \frac{\kappa p_{\triangleright\triangleleft} bU}{c_{\triangleright\triangleleft}}\sum_{i=1}^{3}\left[\int_{x_i}^{x_{i+1}} \frac{d\psi_k(x)}{dx}\psi_j(x)\,\mathrm{d}x\right] + \Omega^2\sum_{i=1}^{3}\left[\rho_i A_i \int_{x_i}^{x_{i+1}} \psi_k(x)\psi_j(x)\,\mathrm{d}x\right] + \Omega\frac{\kappa p_{\triangleright\triangleleft} b}{c_{\triangleright\triangleleft}}\sum_{i=1}^{3}\left[\int_{x_i}^{x_{i+1}} \psi_k(x)\psi_j(x)\,\mathrm{d}x\right]\right) = 0 \tag{79}$$

We introduce the following notations:

$$A_{kj} = \sum_{i=1}^{3}\left[E_i I_i \int_{x_i}^{x_{i+1}} \frac{d^4\psi_k(x)}{dx^4}\psi_j(x)\,\mathrm{d}x\right] \tag{80a}$$

$$B_{kj} = \sum_{i=1}^{3}\left[\int_{x_i}^{x_{i+1}} \frac{d\psi_k(x)}{dx}\psi_j(x)\,\mathrm{d}x\right] \tag{80b}$$

$$C_{kj} = \sum_{i=1}^{3}\left[\rho_i A_i \int_{x_i}^{x_{i+1}} \psi_k(x)\psi_j(x)\,\mathrm{d}x\right] \tag{80c}$$

$$D_{kj} = \sum_{i=1}^{3}\left[\int_{x_i}^{x_{i+1}} \psi_k(x)\psi_j(x)\,\mathrm{d}x\right] \tag{80d}$$

The problem takes the following form:

$$\sum_{k=1}^{n} Q_k\left(A_{kj} + \frac{\kappa p_{\triangleright\triangleleft} bU}{c_{\triangleright\triangleleft}}B_{kj} + \Omega^2 C_{kj} + \Omega\frac{\kappa p_{\triangleright\triangleleft} b}{c_{\triangleright\triangleleft}}D_{kj}\right) = 0 \tag{81}$$

In matrix representation,

$$\left(\boldsymbol{A} + \frac{\kappa p_{\triangleright\triangleleft} bU}{c_{\triangleright\triangleleft}}\boldsymbol{B} + \Omega^2 + \Omega\frac{\kappa p_{\triangleright\triangleleft} b}{c_{\triangleright\triangleleft}}\boldsymbol{D}\right)\boldsymbol{Q} = 0 \tag{82}$$

This system has nontrivial solution only if the following determinant vanishes:

$$\det\left(\boldsymbol{A} + \frac{\kappa p_{\triangleright\triangleleft} bU}{c_{\triangleright\triangleleft}}\boldsymbol{B} + \Omega^2\boldsymbol{C} + \Omega\frac{\kappa p_{\triangleright\triangleleft} b}{c_{\triangleright\triangleleft}}\boldsymbol{D}\right) = 0 \tag{83}$$

To study the dynamic stability, we fix parameters related to the beam, so the only variable of the system is the parameter related to the load: the velocity U. The unknown of the problem is the complex eigenfrequency Ω.

VI. Application of the Modified Galerkin Method

We use the familiar substitution

$$w(x, t) = W(x)e^{\Omega t} \tag{84}$$

Starting from Eq. (4) and using consideration (84), we obtain

Downloaded by UNIVERSITA DI TRENTO on July 20, 2021 | http://arc.aiaa.org | DOI: 10.2514/1.J060631

$$\frac{d^2}{dx^2}\left(E(x)I(x)\frac{d^2W}{dx^2}\right)+\frac{\kappa p_{\triangleright\!\bowtie} bU}{c_{\triangleright\!\bowtie}}\frac{dW}{dx}+\rho(x)A(x)\Omega^2W(x)+\frac{\kappa p_{\triangleright\!\bowtie} b}{c_{\triangleright\!\bowtie}}\Omega W(x)=0 \tag{85}$$

To implement the modified Galerkin method we represent the flexural rigidity and the mass of the system as a generalized function:

$$D(x)=E(x)I(x)=E_1I_1\cdot U(x)+\sum_{j=1}^{2}[(E_{j+1}I_{j+1}-E_jI_j)\cdot U(x-x_j)] \tag{86a}$$

$$M(x)=\rho(x)A(x)=\rho_1A_1\cdot U(x)+\sum_{j=1}^{2}[(\rho_{j+1}A_{j+1}-\rho_jA_j)\cdot U(x-x_j)] \tag{86b}$$

where $U(x-x_j)$ is the unit step function or Heaviside function that has the following properties:

$$U(x-\alpha)=\begin{cases}1 & \text{if } x>\alpha\\ 0 & \text{otherwise}\end{cases} \tag{87a}$$

$$\frac{d}{dx}U(x-\alpha)=\delta(x-\alpha) \tag{87b}$$

$$\frac{d}{dx}\delta(x-\alpha)=\delta'(x-\alpha) \tag{87c}$$

where $\delta(x)$ is the Dirac's delta function, and $\delta'(x-\alpha)$ is the doublet function.

Now, rewriting Eq. (85) with these considerations we obtain

$$\frac{d^2}{dx^2}\left(D(x)\frac{d^2W}{dx^2}\right)+\frac{\kappa p_{\triangleright\!\bowtie} bU}{c_{\triangleright\!\bowtie}}\frac{dW}{dx}+M(x)\Omega^2W(x)+\frac{\kappa p_{\triangleright\!\bowtie} b}{c_{\triangleright\!\bowtie}}\Omega W(x)=0 \tag{88}$$

We evaluate the derivatives to get

$$D(x)\frac{d^4W}{dx^4}+2\frac{d}{dx}D(x)\frac{d^3W}{dx^3}+\frac{d^2}{dx^2}D(x)\frac{d^2W}{dx^2}+\frac{\kappa p_{\triangleright\!\bowtie} bU}{c_{\triangleright\!\bowtie}}\frac{dW}{dx}+M(x)\Omega^2W(x)+\frac{\kappa p_{\triangleright\!\bowtie} b}{c_{\triangleright\!\bowtie}}\Omega W(x)=0 \tag{89}$$

We substitute the approximation in series of $W(x)$ as

$$W(x)=\sum_{k=1}^{n}Q_k\psi_k(x) \tag{90}$$

obtaining

$$\sum_{k=1}^{n}\left[D(x)\frac{d^4\psi_k}{dx^4}+2\frac{d}{dx}D(x)\frac{d^3\psi_k}{dx^3}+\frac{d^2}{dx^2}D(x)\frac{d^2\psi_k}{x^2}+\frac{\kappa p_{\triangleright\!\bowtie} bU}{c_{\triangleright\!\bowtie}}\frac{d\psi_k}{dx}+M(x)\Omega^2\psi_k(x)+\frac{\kappa p_{\triangleright\!\bowtie} b}{c_{\triangleright\!\bowtie}}\Omega\psi_k(x)\right]Q_k=0 \tag{91}$$

We multiply the differential equation by $\psi_j(x)$ and we integrate it from zero to the total length to get

$$\sum_{k=1}^{n}\left[\int_0^L D(x)\frac{d^4\psi_k}{dx^4}\psi_j(x)\,dx+2\int_0^L\frac{d}{dx}D(\xi)\frac{d^3\psi_k}{dx^3}\psi_j(x)\,dx+\int_0^L\frac{d^2}{dx^2}D(x)\frac{d^2\psi_k}{dx^2}\psi_j(x)\,dx+\frac{\kappa p_{\triangleright\!\bowtie} bU}{c_{\triangleright\!\bowtie}}\int_0^L\frac{d\psi_k}{dx}\psi_j(x)\,dx+\Omega^2\int_0^L M(x)\psi_k(x)\psi_j(x)\,dx+\Omega\frac{\kappa p_{\triangleright\!\bowtie} b}{c_{\triangleright\!\bowtie}}\int_0^L\psi_k(x)\psi_j(x)\,dx\right]Q_k=0 \tag{92}$$

Defining

$$A'_{kj}=\int_0^L D(x)\frac{d^4\psi_k}{dx^4}\psi_j(x)\,dx \tag{93a}$$

$$A''_{kj}=\int_0^L\frac{d}{dx}D(x)\frac{d^3\psi_k}{dx^3}\psi_j(x)\,dx \tag{93b}$$

$$A'''_{kj}=\int_0^L\frac{d^2}{dx^2}D()\frac{d^2\psi_k}{dx^2}\psi_j(x)\,dx \tag{93c}$$

$$B_{kj}=\int_0^L\frac{d\psi_k}{dx}\psi_j(x)\,dx \tag{93d}$$

$$C_{kj}=\int_0^L M(x)\psi_k(x)\psi_j(x)\,dx \tag{93e}$$

$$D_{kj}=\int_0^L\psi_k(x)\psi_j(x)dx \tag{93f}$$

we obtain

$$\sum_{k=1}^{n}\left(A'_{kj}+2A''_{kj}+A'''_{kj}+\frac{\kappa p_{\triangleright\!\bowtie} bU}{c_{\triangleright\!\bowtie}}B_{kj}+\Omega^2C_{kj}+\Omega\frac{\kappa p_{\triangleright\!\bowtie} b}{c_{\triangleright\!\bowtie}}D_{kj}\right)Q_k=0 \tag{94}$$

using matrix expression

$$\left(\boldsymbol{A}'+2\boldsymbol{A}''+\boldsymbol{A}'''+\frac{\kappa p_{\triangleright\!\bowtie} bU}{c_{\triangleright\!\bowtie}}\boldsymbol{B}+\Omega^2\boldsymbol{C}+\Omega\frac{\kappa p_{\triangleright\!\bowtie} b}{c_{\triangleright\!\bowtie}}\boldsymbol{D}\right)\boldsymbol{Q}=0 \tag{95}$$

This is a homogeneous system and has a nontrivial solution only if the determinant of the coefficient matrix is equal to zero:

$$\det\left(\boldsymbol{A}'+2\boldsymbol{A}''+\boldsymbol{A}'''+\frac{\kappa p_{\triangleright\!\bowtie} bU}{c_{\triangleright\!\bowtie}}\boldsymbol{B}+\Omega^2\boldsymbol{C}+\Omega\frac{\kappa p_{\triangleright\!\bowtie} b}{c_{\triangleright\!\bowtie}}\boldsymbol{D}\right)=0 \tag{96}$$

We observe that the modified implementation of the Galerkin method leads us to a more detailed stiffness matrix, which is composed of three submatrices $\boldsymbol{A}'$, $\boldsymbol{A}''$, and $\boldsymbol{A}'''$. We also observe that $\boldsymbol{A}'$ is exactly $\boldsymbol{A}$ for the original implementation, so $\boldsymbol{A}''$, and $\boldsymbol{A}'''$; represent the additional terms that donate to the method more precision.

VII. Numerical Example

To study the dynamic stability of a beam into a gas flow, we need to know the parameter of the beam and gas. We take the following data:

$$L_1=L_2=L_3=1\text{ m}$$
$$L=3\text{ m}$$
$$A_1=A_2=A_3=0.01\text{ m}^2$$
$$I_1=I_2=I_3=8.33\times10^{-6}\text{ m}^4$$

The material parameters are given in Table 1.

Downloaded by UNIVERSITA DI TRENTO on July 20, 2021 | http://arc.aiaa.org | DOI: 10.2514/1.J060631

Downloaded by UNIVERSITA DI TRENTO on July 20, 2021 | http://arc.aiaa.org | DOI: 10.2514/1.J060631

Table 1 Material parameters

Parameter	Strong: naval brass	Weak: acrylic
E	$100 \cdot 10^9$ Pa	$3.2 \cdot 10^9$ Pa
ρ	8553 kg/m^3	1180 kg/m^3

Table 2 Gas parameters

Parameter	Value
κ	1.4
$c_{\bowtie}$	340 m/s
$p_{\bowtie}$	$101 \cdot 10^3$ Pa

The gas parameters are given in Table 2.

We discretize the velocity U in 100 points into the interval $U_1 = 0$ and $U_{100} = U_{\max}$ (which is different for every material pattern), and we solve the problem for every speed value into the interval.

Consider the composition S-W-S; in Fig. 2 we have the trend of the imaginary part of the complex frequency Ω in the function of the velocity of gas flow U. In this figure we see that when the speed is equal to zero the two frequencies coincide with the natural frequencies ω_1 and ω_2 because we are in the case without external forces, i.e., free vibrations. When we increase the velocity of the flow, the two frequencies tend to get closer until reaching the coalescence. The velocity in which the coalescence appears is called the "critical velocity" U_{cr} and at that velocity we have the dynamic instability.

In Fig. 3 we have the trend of the real part of the complex frequency Ω in the function of the velocity of gas flow U. In this figure we see that for a low value of the gas velocity the real part of Ω_1 and Ω_2 is the same; the two lines are overlapped. When the speed reaches the value of U_{cr}, the two real parts of the frequencies become different, and we have the instability.

In Fig. 4 we see how the complex frequencies evolve with increasing of gas flow velocity U. The trend, in this plot, is that when the speed is equal to zero the imaginary part of the frequencies is what we have in the natural frequencies and the real part is equal to zero. Increasing the velocity, the two frequencies start to get closer: the imaginary part of Ω_1 increases and the imaginary part of Ω_2 decreases with the real parts of both equal to zero. They reach the coalescence at $U = U_{\text{cr}}$. When we increase again the velocity, the two frequencies diverge: the imaginary part of both increases and the real part of Ω_1 becomes greater than zero and the real part of Ω_2 becomes less than zero.

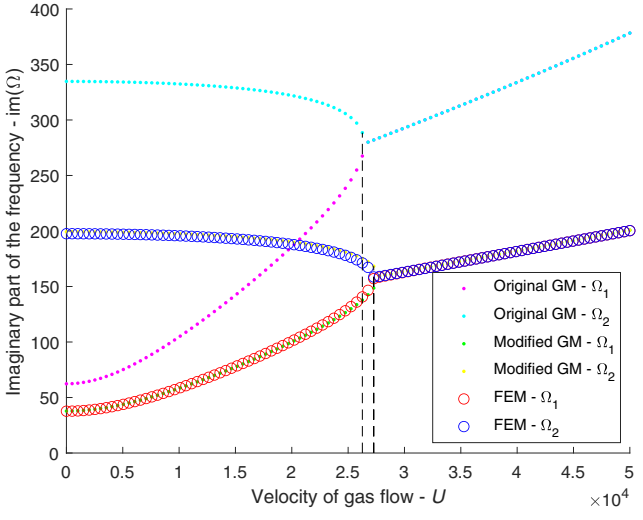

Fig. 2 Imaginary part of the frequency vs velocity of gas flow.

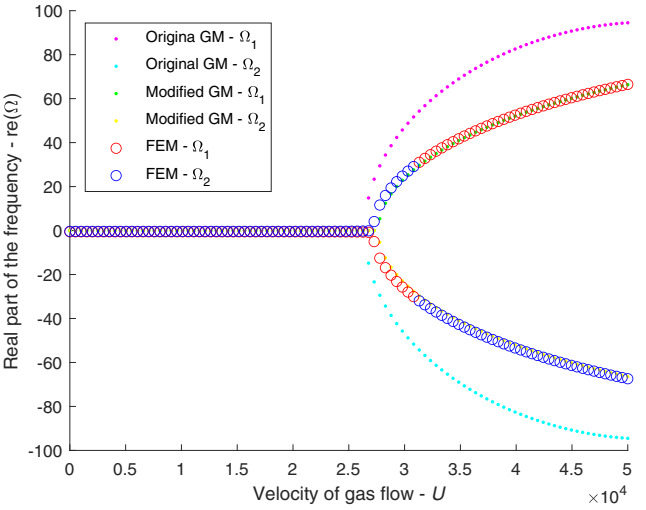

Fig. 3 Real part of the frequency vs velocity of gas flow.

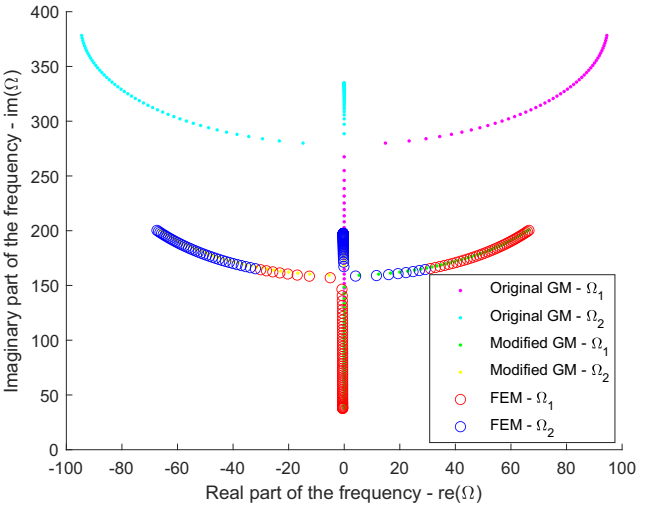

Fig. 4 Imaginary part of the frequency vs real part of the frequency.

As we can see from Figs. 2–4, the trend of the methods is not the same. In particular, the modified Galerkin method tends to the FEM's solution. The original version of the Galerkin method does not tend to the exact solution: it is far everywhere in the plot from FEM's results. In this case we used the Galerkin method up to 300 terms and 3 finite elements for each step: 9 finite elements in total. Table 3 reports the critical velocities obtained with different methods.

The relative error between the critical velocity obtained with both Galerkin methods and the FEM approach is evaluated with the following formula:

$$\varepsilon = \frac{\omega_{\text{Galerkin}} - \omega_{\text{FEM}}}{\omega_{\text{FEM}}} \cdot 100\% \tag{97}$$

The results obtained are shown in Table 4.

As we have shown for the S-W-S material pattern, we report the plots of the solution for the S-S-S case. In Fig. 5 we have shown the

Table 3 Critical velocities by different techniques

Method	Critical velocity U_{cr}, m/s
Original Galerkin method	$2.6263 \cdot 10^4$
Modified Galerkin method	$2.7273 \cdot 10^4$
Finite element method	$2.7273 \cdot 10^4$

Downloaded by UNIVERSITA DI TRENTO on July 20, 2021 | http://arc.aiaa.org | DOI: 10.2514/1.J060631

Table 4 Relative error evaluation

Methods compared	Relative error, %
Original Galerkin method vs FEM	−3.70
Modified Galerkin method vs FEM	0.00

trend of the imaginary part of the complex frequency Ω in the function of the velocity of gas flow U. When the speed is zero, we have the natural frequencies and the critical velocity is represented by the coalescence of the frequencies.

Shown in Fig. 6 is the trend of the real part of the complex frequency Ω in the function of the velocity of gas flow U. This plot is characterized by the coincidence of the frequencies for a low value of the speed and the instability is reached when the frequencies become different.

In Fig. 7 we see how the complex frequencies evolve with increasing gas flow velocity U. When the speed is zero, the imaginary part of the frequencies is the natural frequency. Increasing velocity flow brings the imaginary part closer and the beam became unstable when the critical velocity is reached: here we have the divergence of the frequencies.

As we can see from Figs. 5–7 that all the approaches used lead us to the same critical velocity, and all the methods in each plot are perfectly overlapped. In particular, the two different implementations of the Galerkin method yield the same results because the beams are homogeneous and uniform, and Eq. (95) becomes equal to Eq. (82)

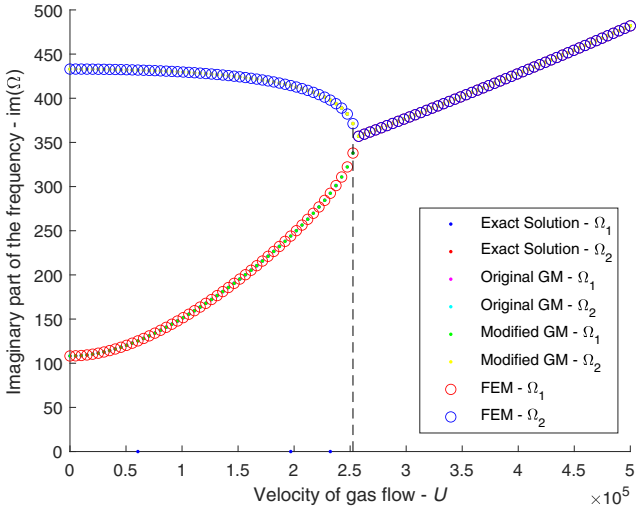

Fig. 5 Imaginary part of the frequency vs velocity of gas flow.

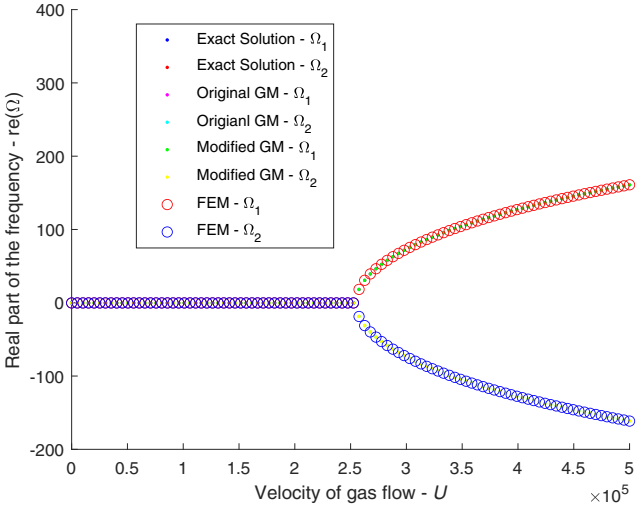

Fig. 6 Real part of the frequency vs velocity of gas flow.

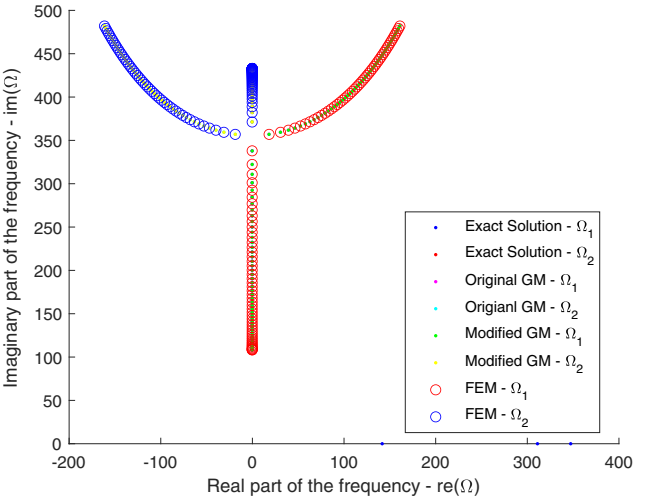

Fig. 7 Imaginary part of the frequency vs real part of the frequency.

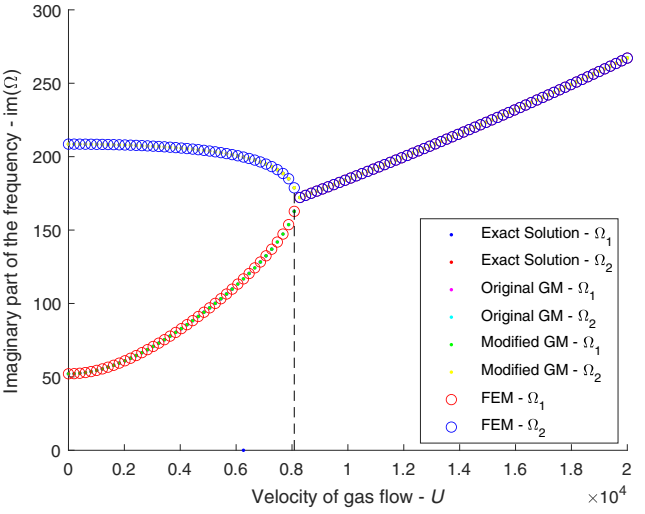

Fig. 8 Imaginary part of the frequency vs velocity of gas flow.

because the two additional terms are equal to zero because there are no steps in this beam. In this case we used the Galerkin method until 10 terms and 3 finite elements for each step: nine 9 elements in total.

Table 5 reports the critical velocities obtained with different methods.

The relative error between the critical velocity obtained with both Galerkin methods and with the FEM approach compared with the exact solution is evaluated with the following formula:

$$\varepsilon = \frac{\omega - \omega_{\text{Exact}}}{\omega_{\text{Exact}}} \cdot 100\% \tag{98}$$

The results obtained are shown in Table 6.

Consider now the uniform beam that can be designated as a W-W-W beam with each part being made of the weak material. Following the same approach of S-W-S and S-S-S material patterns, we have

Table 5 Critical velocities furnished by different methods

Method	Critical velocity U_{cr}, m/s
Exact solution	$2.5253 \cdot 10^5$
Original Galerkin method	$2.5253 \cdot 10^5$
Modified Galerkin method	$2.5253 \cdot 10^5$
Finite element method	$2.5253 \cdot 10^5$

Table 6 Relative errors in comparison with exact solution

Methods compared	Relative error, %
Original Galerkin method vs exact solution	0.00
Modified Galerkin method vs exact solution	0.00
Finite Element method vs exact solution	0.00

shown the solution plots. In Fig. 8 we have the trend of the imaginary part of the complex frequency Ω in the function of the velocity of gas flow U.

In Fig. 9 we have the trend of the real part of the complex frequency Ω in the function of the velocity of gas flow U.

In Fig. 10 we see how the complex frequencies evolve with increasing gas flow velocity U.

Figures 8–10 lead us the following considerations: all the approaches used lead us to the same critical velocity. According to the S-S-S case, for the homogeneous and uniform beam there are no differences between the original and the modified versions of Galerkin method implementations.

Table 7 shows the critical velocities obtained with different methods.

The relative error between the critical velocity obtained with both Galerkin methods and with the FEM approach compared with the exact solution is evaluated with the following formula:

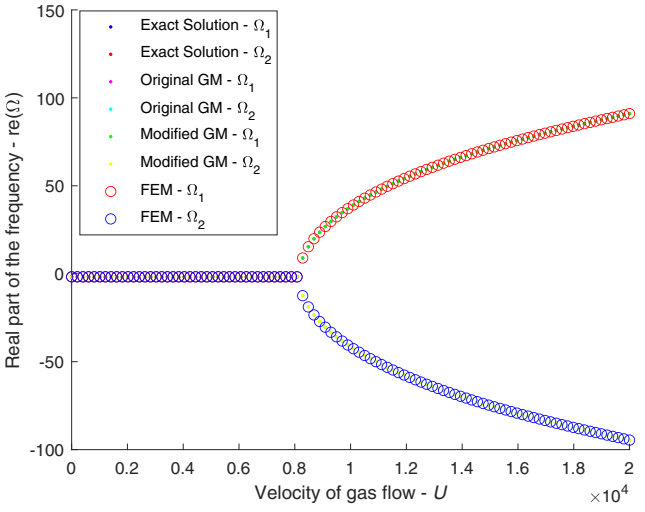

Fig. 9 Real part of the frequency vs velocity of gas flow.

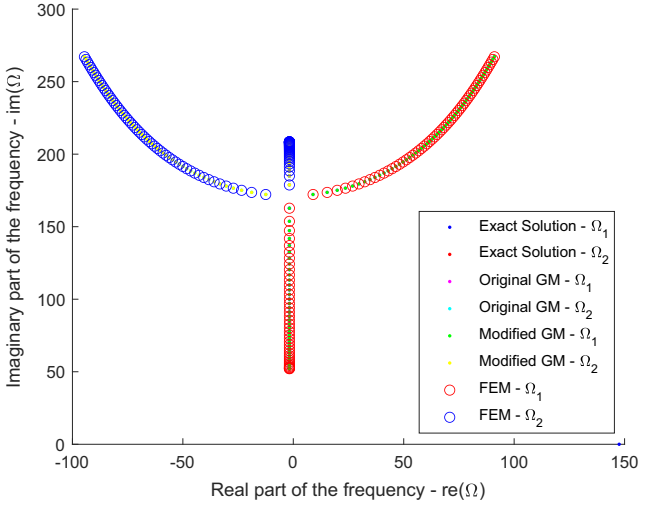

Fig. 10 Imaginary part of the frequency vs real part of the frequency.

Table 7 Critical velocities evaluated by different methods

Method	Critical velocity U_{cr}, m/s
Exact solution	$8.0808 \cdot 10^3$
Original Galerkin method	$8.0808 \cdot 10^3$
Modified Galerkin method	$8.0808 \cdot 10^3$
Finite Element method	$8.0808 \cdot 10^3$

Table 8 Relative errors

Methods compared	Relative error, %
Original Galerkin method vs exact solution	0.00
Modified Galerkin method vs exact solution	0.00
Finite Element method vs exact solution	0.00

$$\varepsilon = \frac{\omega - \omega_{\text{Exact}}}{\omega_{\text{Exact}}} \cdot 100\% \tag{99}$$

The results obtained are shown in Table 8.

VIII. Conclusions

This study has investigated the dynamic stability of three different combinations of materials keeping constant the geometric features of the beam. The following conclusions are obtained: first of all, the modified Galerkin method tends to the finite element solution for the inhomogeneous case in contrast with the original implementation, which does not. Secondly, original and modified Galerkin methods tend to the same solution in the homogeneous case. Thirdly, original and modified Galerkin methods in the inhomogeneous case require many more terms (namely, 300) than the in modified Galerkin method in the homogeneous case, where 10 terms are sufficient. In conclusion, the modified Galerkin method turns out to be an effective means of determining critical flutter velocity.

References

[1] Bisplinghoff, R. L., Ashley, H., and Halfman, R. L., *Aeroelasticity*, Addison-Wesley, Boston, 1955, Chap. 9.

[2] Fung, Y. C., *An Introduction to the Theory of Aeroelasticity*, Wiley, New York, 1955, Chaps. 5, 6, and 7.

[3] Bolotin, V. V., *Nonconservative Problems of the Theory of Elastic Stability*, Macmillan, New York, 1963, Chap. 4.

[4] Försching, H. W., *Grundlagen der Aeroelastik [Fundamentals of Aeroelasticity]*, Springer, Berlin, 1974, Chap. 4 (in German).

[5] Dowell, E. H., *Aeroelasticity of Plates and Shells*, Noordhoff International, Leyden, The Netherlands, 1975, Chap. 1.

[6] Librescu, L., *Elastostatics and Kinetics of Anisotropic and Heterogeneous Shell-Type Structures*, Noordhoff International, Leyden, The Netherlands, 1976, Chap. 5.

[7] Starossek, U., *Brückendynamik: Winderregte Schwingungen von Seilbrücken [Bridge Dynamics: Wind-Induced Vibrations of Rope Bridges]*, Vieweg, Braunschweig, Germany, 1992, Chap. 5 (in German).

[8] Hodges, D. H., and Pierce, G. A., *Introduction to Structural Dynamics and Aeroelasticity*, Cambridge Univ. Press, Cambridge, England, U.K., 2002, Chap. 5.

[9] Wright, J. R., and Cooper, J. E., *Introduction to Aircraft Aeroelasticity and Loads*, Wiley, New York, 2007, Chap. 10.

[10] Algazin, S. D., and Kijko, I. A., *Aeroelastic Vibrations and Stability of Plates and Shells*, Walter de Gruyter Gmbh, Berlin, 2015, Chap. 1.

[11] Bhat, R. B., *Principles of Aeroelasticity*, CRC Press, Boca Raton, FL, 2016, Chap. 9.

[12] Dowell, E. H., *A Modern Course in Aeroelasticity*, 5th ed., Springer, Cham, Switzerland, 2015, Chap. 4.

[13] Dowell, E. H., "Panel Flutter—A Review of the Aeroelastic Stability of Plates and Shells," *AIAA Journal*, Vol. 8, No. 3, 1970, pp. 385–399. https://doi.org/10.2514/3.5680

[14] Novichkov, Y. N., "Flutter of Plates and Shells," *Advances in Science and Technology: Mechanics of Deformable Solids*, Vol. 11, 1978,

Downloaded by UNIVERSITA DI TRENTO on July 20, 2021 | http://arc.aiaa.org | DOI: 10.2514/1.J060631

pp. 67–122 (in Russian), https://scholar.google.com/scholar_lookup?title=Flutter%20of%20plates%20and%20shells&publication_year=1978&author=Yu.N.%20Novichkov.
[15] Friedmann, P. P., "Renaissance of Aeroelasticity and Its Future," *Journal of Aircraft*, Vol. 36, No. 1, 1999, pp. 105–121. https://doi.org/10.2514/2.2418
[16] Livne, E., "Future of Airplane Aeroelasticity," *Journal of Aircraft*, Vol. 40, No. 6, 2003, pp. 1066–1092. https://doi.org/10.2514/2.7218
[17] Pettit, C. L., "Uncertainty Quantification in Aeroelasticity: Recent Results and Research Challenges," *Journal of Aircraft*, Vol. 41, No. 5, 2004, pp. 1217–1229. https://doi.org/10.2514/1.3961
[18] Dowell, E., "Some Recent Advances in Nonlinear Aeroelasticity: Fluid-Structure Interaction in the 21st Century," *Proceedings of the 51st AIAA/ASME/ASCE/AHS/ASC Structures, Structural Dynamics, and Materials Conference*, AIAA Paper 2010-3137, 2010. https://doi.org/10.2514/6.2010-3137
[19] Beran, P., Stanford, B., and Schrock, C., "Uncertainty Quantification in Aeroelasticity," *Annual Review of Fluid Mechanics*, Vol. 49, Jan. 2017, pp. 361–386. https://doi.org/10.1146/annurev-fluid-122414-034441
[20] Aßmus, M., Bergmann, S., Naumenko, K., and Altenbach, H., "Mechanical Behavior of Photovoltaic Composite Structures: A Parameter Study on the Influence of Geometric Dimensions and Material Properties Under Static Loading," *Composites Communications*, Vol. 5, Dec. 2017, pp. 23–26.
[21] Viverge, K., Boutin, C., and Sallet, F., "Model of Highly Contrasted Plates Versus Experiments on Laminated Glass," *International Journal of Solids and Structures*, Vol. 102, Dec. 2016, pp. 238–258. https://doi.org/10.1016/j.ijsolstr.2016.09.035
[22] Qin, Y., Wang, X., and Wang, Z. L., "Microfibre—Nanowire Hybrid Structure for Energy Scavenging," *Nature*, Vol. 451, No. 7180, 2008, pp. 809–813. https://doi.org/10.1038/nature06601
[23] Ruzzene, M., and Baz, A., "Attenuation and Localization of Wave Propagation in Periodic Rods Using Shape Memory Inserts," *Smart Materials and Structures*, Vol. 9, No. 6, 2000, p. 805.
[24] Martin, T. P., Layman, C. N., Moore, K. M., and Orris, G. J., "Elastic Shells with High-Contrast Material Properties as Acoustic Metamaterial Components," *Physical Review B*, Vol. 85, No. 16, 2012, Paper 161103. https://doi.org/10.1103/PhysRevB.85.161103
[25] Kaplunov, J., Prikazchikov, D., and Sergushova, O., "Multi-Parametric Analysis of the Lowest Natural Frequencies of Strongly Inhomogeneous Elastic Rods," *Journal of Sound and Vibration*, Vol. 366, March 2016, pp. 264–276. https://doi.org/10.1016/j.jsv.2015.12.008
[26] Kudaibergenov, A., Nobili, A., and Prikazchikova, L., "On Low-Frequency Vibrations of a Composite String with Contrast Properties for Energy Scavenging Fabric Devices," *Journal of Mechanics of Materials and Structures*, Vol. 11, No. 3, 2016, pp. 231–243. https://doi.org/10.2140/jomms.2016.11.231
[27] Kaplunov, J., Prikazchikov, D. A., Prikazchikova, L. A., and Sergushova, O., "The Lowest Vibration Spectra of Multi-Component Structures with Contrast Material Properties," *Journal of Sound and Vibration*, Vol. 445, April 2019, pp. 132–147. https://doi.org/10.1016/j.jsv.2019.01.013
[28] Şahin, O., Erbaş, B., Kaplunov, J., and Savšek, T., "The Lowest Vibration Modes of an Elastic Beam Composed of Alternating Stiff and Soft Components," *Archive of Applied Mechanics*, Vol. 90, No. 2, 2020, pp. 319–352. https://doi.org/10.1007/s00419-019-01612-2
[29] Li, Y. W., Elishakoff, I., and Starnes, J. H., Jr., "Buckling Mode Localization in a Multi-Span Periodic Structure with a Disorder in a Single Span," *Chaos, Solitons & Fractals*, Vol. 5, No. 6, 1995, pp. 955–969. https://doi.org/10.1016/0960-0779(94)00211-8
[30] Xie, W. C., and Elishakoff, I., "Buckling Mode Localization in Rib-Stiffened Plates with Misplaced Stiffeners—Kantorovich Approach," *Chaos, Solitons & Fractals*, Vol. 11, No. 10, 2000, pp. 1559–1574. https://doi.org/10.1016/S0960-0779(99)00078-8
[31] Zingales, M., and Elishakoff, I., "Localization of the Bending Response in Presence of Axial Load," *International Journal of Solids and Structures*, Vol. 37, No. 45, 2000, pp. 6739–6753. https://doi.org/10.1016/S0020-7683(99)00282-6
[32] Elishakoff, I., Li, Y., and Starnes, J. H., Jr., *Non-Classical Problems in the Theory of Elastic Stability*, Cambridge Univ. Press, Cambridge, England, U.K., 2001, Chap. 1.
[33] Dugundji, J., Dowell, E., and Perkin, B., "Subsonic Flutter of Panels on Continuous Elastic Foundations," *AIAA Journal*, Vol. 1, No. 5, 1963, pp. 1146–1154. https://doi.org/10.2514/3.1738
[34] Fung, Y. C., "Some Recent Contributions to Panel Flutter Research," *AIAA Journal*, Vol. 1, No. 4, 1963, pp. 898–909. https://doi.org/10.2514/3.1661
[35] Kaza, K. R. V., and Kielb, R. E., "Flutter and Response of a Mistuned Cascade in Incompressible Flow," *AIAA Journal*, Vol. 20, No. 8, 1982, pp. 1120–1127. https://doi.org/10.2514/3.51172
[36] Parks, P. C., "A Stability Criterion for Panel Flutter via the Second Method of Liapunov," *AIAA Journal*, Vol. 4, No. 1, 1966, pp. 175–177. https://doi.org/10.2514/3.3412
[37] Dugundji, J., "Theoretical Considerations of Panel Flutter at High Supersonic Mach Numbers," *AIAA Journal*, Vol. 4, No. 7, 1966, pp. 1257–1266. https://doi.org/10.2514/3.3657
[38] Gwin, L. B., and Taylor, R. F., "A General Method for Flutter Optimization," *AIAA Journal*, Vol. 11, No. 12, 1973, pp. 1613–1617. https://doi.org/10.2514/3.50657
[39] Pidaparti, R. M. V., and Yang, H. T., "Supersonic Flutter Analysis of Composite Plates and Shells," *AIAA Journal*, Vol. 31, No. 6, 1993, pp. 1109–1117. https://doi.org/10.2514/3.11735
[40] Zhang, W. W., Ye, Z. Y., Zhang, C. A., and Liu, F., "Supersonic Flutter Analysis Based on a Local Piston Theory," *AIAA Journal*, Vol. 47, No. 10, 2009, pp. 2321–2328. https://doi.org/10.2514/1.37750
[41] Dowell, E. H., and Bendiksen, O., "Panel Flutter," *Encyclopedia of Aerospace Engineering*, Oddvar, 2010. https://doi.org/10.1002/9780470686652.eae152
[42] Elishakoff, I., and Khromatoff, V., "Statistical Analysis of the Vibrations of a Panel in a Supersonic Flow," *Mechanics of Solids*, Vol. 5, No. 4, 1971, pp. 41–45.
[43] Elishakoff, I., "Flutter and Random Vibration in Plates," *Stochastic Problems in Dynamics*, edited by B. L. Clarkson, Pitman Press, London, 1977, pp. 390–411.
[44] Hashimoto, A., Aoyama, T., and Nakamura, Y., "Effects of Turbulent Boundary Layer on Panel Flutter," *AIAA Journal*, Vol. 47, No. 12, 2009, pp. 2785–2791. https://doi.org/10.2514/1.35786
[45] Veletsos, A. S., and Newmark, N. M., "A Simple Approximation of the Fundamental Frequencies of Two-Span and Three-Span Continuous Beams," Univ. of Illinois, Rept. AD29637, Urbana, IL, 1954, http://hdl.handle.net/2142/13956.
[46] Makhortykh, Z. K., "Vibrations of a Two-Span Plate in Vacuum," *Inzhenernyi Sbornik*, Vol. 1, No. 3, 1961, pp. 102–106 (in Russian).
[47] Gorman, D. J., "Free Lateral Vibration Analysis of Double-Span Uniform Beams," *International Journal of Mechanical Sciences*, Vol. 16, No. 6, 1974, pp. 345–351. https://doi.org/10.1016/0020-7403(74)90008-3
[48] Makhortykh, Z. K., "Stability of Multispan Plate Moving in a Gas," *Mashinostroenie*, Vol. 2, No. 19559, 1959, pp. 174–177 (in Russian).
[49] Makhortykh, Z. K., "Vibrations of Two-Span Panel in Gas Flow," *Inzhenernyi Sbornik*, Vol. 28, 1960, pp. 51–54 (in Russian).
[50] Rodden, W. P., "Flutter of Multibay Panels at Supersonic Speeds," *AIAA Journal*, Vol. 2, No. 8, 1964, pp. 1476–1478. https://doi.org/10.2514/3.2614
[51] Dowell, E. H., "Flutter of Multibay Panels at High Supersonic Speeds," *AIAA Journal*, Vol. 2, No. 10, 1967, pp. 1805–1814. https://doi.org/10.2514/3.2669
[52] Dowell, E. H., "On the Flutter of Multibay Panels at Low Supersonic Speeds," *AIAA Journal*, Vol. 5, No. 5, 1967, pp. 1032–1033. https://doi.org/10.2514/3.4125
[53] Song, Z. G., and Li, F. M., "Vibration and Aeroelastic Properties of Ordered and Disordered Two-Span Panels in Supersonic Airflow," *International Journal of Mechanical Sciences*, Vol. 81, April 2014, pp. 65–72. https://doi.org/10.1016/j.ijmecsci.2014.02.004
[54] Marzani, A., Mazzotti, M., Viola, E., Vittori, P., and Elishakoff, I., "FEM Formulation for Dynamic Instability of Fluid-Conveying Pipe on Non-uniform Elastic Foundation," *Mechanics Based Design of Structures and Machines*, Vol. 40, No. 1, 2012, pp. 83–95. https://doi.org/10.1080/15397734.2011.618443
[55] Olson, M. D., "Finite Elements Applied to Panel Flutter," *AIAA Journal*, Vol. 5, No. 12, 1967, pp. 2267–2270. https://doi.org/10.2514/3.4422
[56] Olson, L. G., and Jamison, D., "Application of a General-Purpose Finite Element Method to Elastic Pipes Conveying Fluid," *Journal of Fluids*

Downloaded by UNIVERSITA DI TRENTO on July 20, 2021 | http://arc.aiaa.org | DOI: 10.2514/1.J060631

and Structures, Vol. 11, No. 2, 1997, pp. 207–222.
https://doi.org/10.1006/jfls.1996.0073

[57] Kock, E., and Olson, L., "Fluid–Structure Interaction Analysis by the Finite Element Method—A Variational Approach," *International Journal for Numerical Methods in Engineering*, Vol. 31, No. 3, 1991, pp. 463–491.
https://doi.org/10.1002/nme.1620310305

[58] Pramila, A., Laukkanen, J., and Liukkonen, S., "Dynamics and Stability of Short Fluid-Conveying Timoshenko Element Pipes," *Journal of Sound and Vibration*, Vol. 144, No. 3, 1991, pp. 421–425.
https://doi.org/10.1016/0022-460X(91)90561-W

[59] Ryu, S. U., Sugiyama, Y., and Ryu, B. J., "Eigenvalue Branches and Modes for Flutter of Cantilevered Pipes Conveying Fluid," *Computers & Structures*, Vol. 80, Nos. 14–15, 2002, pp. 1231–1241.
https://doi.org/10.1016/S0045-7949(02)00083-4

S. Shin
Associate Editor

Downloaded by UNIVERSITA DI TRENTO on July 20, 2021 | http://arc.aiaa.org | DOI: 10.2514/1.J060631